

# 1 atems: Analysis tools for TEM images of 2 carbonaceous particles

3 **Timothy A Sipkens**  <sup>1,2</sup>¶, **Ramin Dastanpour**<sup>1</sup>, **Una Trivanovic**  <sup>1</sup>, **Hamed Nikookar**<sup>1</sup>, and **Steven N. Rogak**  <sup>1</sup>

5 **1** Mechanical Engineering, University of British Columbia, Canada **2** Metrology Research Centre,  
6 National Research Council Canada, Canada ¶ Corresponding author

DOI: [10.xxxxxx/draft](https://doi.org/10.xxxxxx/draft)

## Software

- 7 ▪ [Review](#) ↗
- 8 ▪ [Repository](#) ↗
- 9 ▪ [Archive](#) ↗

---

Editor: [Open Journals](#) ↗

Reviewers:

- [@openjournals](#)

Submitted: 01 January 1970

Published: unpublished

## License

Authors of papers retain copyright and release the work under a Creative Commons Attribution 4.0 International License ([CC BY 4.0](#)).<sup>18</sup>

## 7 Introduction

8 Soot, carbon black, and other carbonaceous particles have important climate, health, and technological impacts that depend on their morphology. These particles have complex shapes composed of a collection of small, primary particles in fractal arrangements, as shown in **Figure 1a**. Transmission electron microscopy (TEM) images of these particles allow for detailed information about particle morphology that is unavailable in other characterization techniques. However, extracting this information requires image analysis across a statistically-significant number of particles, with the quality of conclusions improving as the number of characterized particles increases. For instance, Kelesidis et al. (2020) suggested quantifying at least 400 primary particles per experimental condition in a premixed flame to get an accurate average primary particle diameter from manually drawing ellipses (that study counted 800 primary particles). In the broader literature, a few hundred particles per condition seems to be standard, with other authors having employed between 150 and 400 particles per condition (Liati et al., 2014; Marhaba et al., 2019; Trivanovic et al., 2019, 2020), depending on the type of analysis. For multiple conditions, this can quickly expand to over 1000 particles. This characterization is often done manually, which at a minimum of several minutes per aggregate, is incredibly labour intensive. Unfortunately, the low contrast (carbonaceous particles on carbon films) and complex particle morphology of common carbonaceous particles makes automated analysis challenging, requiring unique analysis methods over those developed for traditional TEM image analysis of many engineered nanomaterials (Schneider et al., 2012). At the same time, existing automated methods across the literature are typically only applied to data from a single laboratory, with few exceptions (Anderson et al., 2017; Sipkens et al., 2021). This limits comparability between laboratories (Sipkens et al., 2023).

30 The objective of atems is to provide a suite of open source analysis tools (largely in Matlab) for TEM image analysis that are specifically designed for soot and related carbonaceous particles (e.g., tarballs). This codebase started as a manual analysis code by Dastanpour & Rogak (2014), with the first automated methods added by Dastanpour et al. (2016). The current, 31 open source version has been streamlined and expanded to include a larger suite of automated 32 analysis methods from the literature, as detailed in the following section. In this regard, a key 33 contribution of this codebase is to provide open source implementations of multiple analysis 34 methods spanning a range of laboratories. This codebase places these methods in the same 35 framework, with the goal of enabling intercomparisons of analysis routines across a range of 36 data.

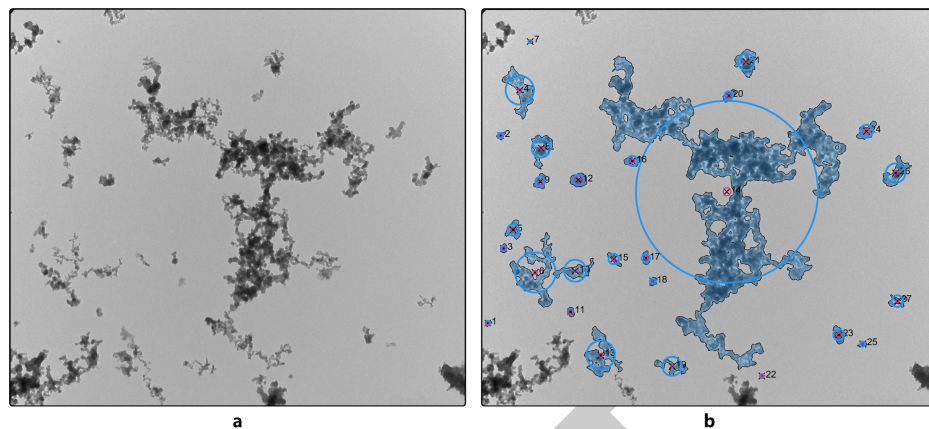


**Figure 1:** Sample TEM image of soot demonstrating the aggregate structure, where **a** is an unlabeled image containing soot aggregates and **b** is that same image with the aggregates labeled.

## 40 Methods

41 After loading images (with an automated method provided for doing so), analysis involves two  
 42 major steps.

43 The first step is segmentation of the aggregates from their background. Available methods  
 44 include the slider-based manual approach of Dastanpour & Rogak (2014); the common Otsu  
 45 method; a modification of Otsu by Dastanpour et al. (2016) that employs morphological  
 46 operations to improve segmentation; the  $k$ -means approach of Sipkens & Rogak (2021); and  
 47 carboseg, which is the convolutional neural network (CNN) approach from Sipkens et al.  
 48 (2021). Functionality is also available to prepare (e.g., read and crop image footers) and  
 49 export images for external analysis, prior to reading the images in for subsequent analysis.  
 50 This enables external extensions, such as the WEKA segmentation method of Altenhoff et  
 51 al. (2020). Tools are then available to compute aggregate projected area, perimeter, and  
 52 circularity, among other properties. A sampling of segmentations produced by these methods  
 53 is presented in Figure 2.

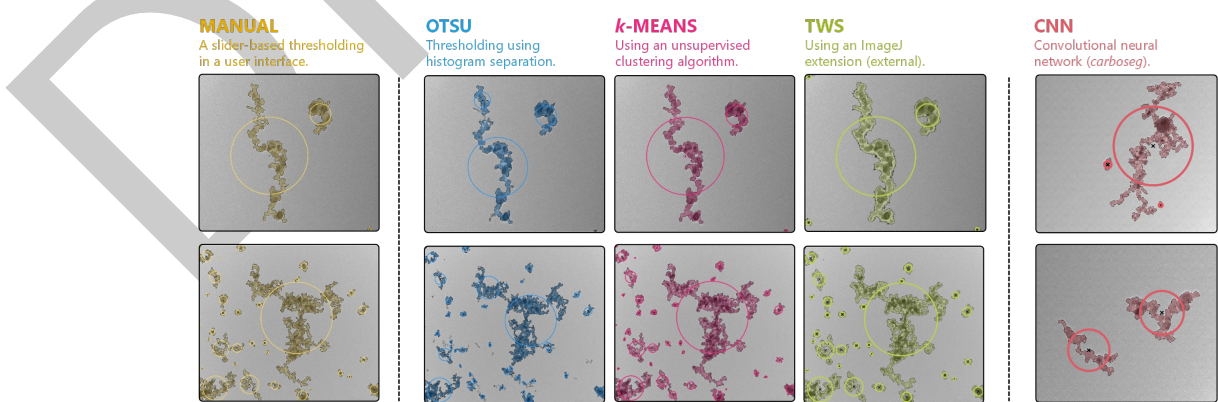


**Figure 2:** Sample segmentations across a range of methods available in this code. The manual method corresponds to an updated version of the code development by Dastanpour et al. (2016). The Otsu segmentation is standard Otsu, without any adaptations. The  $k$ -means method is that described by Sipkens & Rogak (2021). TWS refers to trainable WEKA segmentation based on the method described by Altenhoff et al. (2020), which makes use of the code enabling external extensions. These first four panels correspond to images from Sipkens & Rogak (2021). The final panel corresponds to the convolutional neural network method described by Sipkens et al. (2021).

54 Second, this code works to identify primary particles, that is the small, roughly circular  
55 structures inside the aggregates. Available methods include a updated version of the Euclidean  
56 distance mapping–surface-based scale analysis (EDM-SBS) of Bescond et al. (2014), converted  
57 from SciLab to Matlab in association with Sipkens et al. (2021) (functionality between the two  
58 languages resulted in minor differences); the Euclidean distance mapping–watershed (EDM-WS)  
59 method of De Temmerman et al. (2014); the pair correlation method (PCM) of Dastanpour  
60 et al. (2016); the Hough transform method of Kook et al. (2016); and the Hough transform  
61 method of Altenhoff et al. (2020).

62 General plotting and other utilities (`tools.*`) are provided to enable further analysis and  
63 visualization (e.g., as in [Figure 1b](#) and [Figure 2](#)).

## 64 Use

65 This code has been used in a number of studies in the literature. This code was used by  
66 Sipkens et al. (2021) to compare multiple segmentation and primary particle analysis methods.  
67 The code was also used by Trivanovic et al. (2019), Kheirkhah et al. (2020), and Trivanovic  
68 et al. (2020) to perform image analysis of marine engine and flare soot. The *k*-means method  
69 in this code (Sipkens & Rogak, 2021) was also employed for soot by Li (2022).

## 70 Acknowledgements

71 We wish to acknowledge related code released in association with some of the cited work.  
72 These including Matlab code provided in Kook et al. (2016) and [SciLab code](#) released in  
73 association with Bescond et al. (2014). The code from Altenhoff et al. (2020) was provided  
74 by the authors and adapted to the present format.

75 We also wish to acknowledge funding by the Canadian Council of the Arts (Killam Fellowship),  
76 the Natural Sciences and Engineering Research Council of Canada (NSERC), and Transport  
77 Canada.

## 78 References

- 79 Altenhoff, M., Aßmann, S., Teige, C., Huber, F. J. T., & Will, S. (2020). An optimi-  
80 zed evaluation strategy for a comprehensive morphological soot nanoparticle aggre-  
81 gation characterization by electron microscopy. *Journal of Aerosol Science*, 139, 105470.  
82 <https://doi.org/10.1016/j.jaerosci.2019.105470>
- 83 Anderson, P. M., Guo, H., & Sunderland, P. B. (2017). Repeatability and reproducibility  
84 of TEM soot primary particle size measurements and comparison of automated methods.  
85 *Journal of Aerosol Science*, 114, 317–326. <https://doi.org/10.1016/j.jaerosci.2017.10.002>
- 86 Bescond, A., Yon, J., Ouf, F. X., Ferry, D., Delhaye, D., Gaffié, D., Coppalle, A., & Rozé, C.  
87 (2014). Automated determination of aggregate primary particle size distribution by TEM  
88 Image Analysis: Application to soot. *Aerosol Science and Technology*, 48(8), 831–841.  
89 <https://doi.org/10.1080/02786826.2014.932896>
- 90 Dastanpour, R., Boone, J. M., & Rogak, S. N. (2016). Automated primary particle sizing  
91 of nanoparticle aggregates by TEM image analysis. *Powder Technology*, 295, 218–224.  
92 <https://doi.org/10.1016/j.powtec.2016.03.027>
- 93 Dastanpour, R., & Rogak, S. N. (2014). Observations of a correlation between primary particle  
94 and aggregate size for soot particles. *Aerosol Science and Technology*, 48(10), 1043–1049.  
95 <https://doi.org/10.1080/02786826.2014.955565>

- 96 De Temmerman, P.-J., Verleysen, E., Lammertyn, J., & Mast, J. (2014). Semi-automatic size  
97 measurement of primary particles in aggregated nanomaterials by transmission electron  
98 microscopy. *Powder Technology*, 261, 191–200. <https://doi.org/10.1016/j.powtec.2014.04.040>
- 100 Kelesidis, G. A., Kholghy, M. R., Zuercher, J., Robertz, J., Allemand, M., Duric, A., & Pratsinis,  
101 S. E. (2020). Light scattering from nanoparticle agglomerates. *Powder Technology*, 365,  
102 52–59. <https://doi.org/10.1016/j.powtec.2019.02.003>
- 103 Kheirkhah, P., Baldelli, A., Kirchen, P., & Rogak, S. (2020). Development and validation of  
104 a multi-angle light scattering method for fast engine soot mass and size measurements.  
105 *Aerosol Science and Technology*, 54(9), 1083–1101. <https://doi.org/10.1080/02786826.2020.1758623>
- 107 Kook, S., Zhang, R., Chan, Q. N., Aizawa, T., Kondo, K., Pickett, L. M., Cenker, E.,  
108 Bruneaux, G., Andersson, O., Pagels, J., & Z., N. E. (2016). Automated detection of  
109 primary particles from transmission electron microscope (TEM) images of soot aggregates  
110 in diesel engine environments. *SAE International Journal of Engines*, 9(1), 279–296.  
111 <https://doi.org/10.4271/2015-01-1991>
- 112 Li, Y. (2022). *Flame and smoke characterization in reduced gravity for enhanced spacecraft  
113 safety* [PhD thesis]. Sorbonne Université.
- 114 Lati, A., Brem, B. T., Durdina, L., Vögltli, M., Arroyo Rojas Dasilva, Y., Dimopoulos  
115 Eggenschwiler, P., & Wang, J. (2014). Electron microscopic study of soot particulate  
116 matter emissions from aircraft turbine engines. *Environmental Science & Technology*,  
117 48(18), 10975–10983. <https://doi.org/10.1021/es501809b>
- 118 Marhaba, I., Ferry, D., Laffon, C., Regier, T. Z., Ouf, F.-X., & Parent, P. (2019). Aircraft  
119 and MiniCAST soot at the nanoscale. *Combustion and Flame*, 204, 278–289. <https://doi.org/10.1016/j.combustflame.2019.03.018>
- 121 Schneider, C. A., Rasband, W. S., & Eliceiri, K. W. (2012). NIH image to ImageJ: 25 years of  
122 image analysis. *Nature Methods*, 9(7), 671–675. <https://doi.org/10.1038/nmeth.2089>
- 123 Sipkens, T. A., Boies, A., Corbin, J. C., Chakrabarty, R. K., Olfert, J. S., & Rogak, S. N.  
124 (2023). Overview of methods to characterize the mass, size, and morphology of soot.  
125 *Journal of Aerosol Science*, 173, 106211. <https://doi.org/10.1016/j.jaerosci.2023.106211>
- 126 Sipkens, T. A., Frei, M., Baldelli, A., Kirchen, P., Kruis, F. E., & Rogak, S. N. (2021). Char-  
127 acterizing soot in TEM images using a convolutional neural network. *Powder Technology*,  
128 387, 313–324. <https://doi.org/10.1016/j.powtec.2021.04.026>
- 129 Sipkens, T. A., & Rogak, S. N. (2021). Using k-means to identify soot aggregates in  
130 transmission electron microscopy images. *Journal of Aerosol Science*, 152, 105699. <https://doi.org/10.1016/j.jaerosci.2020.105699>
- 132 Trivanovic, U., Corbin, J. C., Baldelli, A., Peng, W., Yang, J., Kirchen, P., Miller, J. W.,  
133 Lobo, P., Gagné, S., & Rogak, S. N. (2019). Size and morphology of soot produced by  
134 a dual-fuel marine engine. *Journal of Aerosol Science*, 138, 105448. <https://doi.org/10.1016/j.jaerosci.2019.105448>
- 136 Trivanovic, U., Sipkens, T. A., Kazemimanesh, M., Baldelli, A., Jefferson, A. M., Conrad, B.  
137 M., Johnson, M. R., Corbin, J. C., Olfert, J. S., & Rogak, S. N. (2020). Morphology and  
138 size of soot from gas flares as a function of fuel and water addition. *Fuel*, 279, 118478.  
139 <https://doi.org/10.1016/j.fuel.2020.118478>